BB

LPC CAEN

sw9515

LABORATOIRE DE PHYSIQUE CORPUSCULAIRE

ISMRA - Boulevard Maréchal Juin - 14050 CAEN CEDEX - FRANCE

Evolution of reaction mechanisms in symmetrical nucleus-nucleus collisions as a function of the total mass of the sytem from 25 to 74 Mev/u

V. Métivier, R. Bougault, J.L. Charvet, D. Cussol, D. Durand, R. Laforest, J.F. Lecolley, O. Lopez, J.C. Steckmeyer, B.Tamain, E.Vient, G. Auger, Ch.O. Bacri, A. Benkirane, J. Benlliure, B. Berthier, B. Borderie, P. Box, R. Brou, Y. Cassagnou, A. Chbihi, J. Colin, R. Dayras, E. De Filippo, A. Demeyer, P. Ecomard, P. Eudes, A. Genoux-Lubain, D. Gourio, D. Guinet, L. Lakehal-Ayat, P. Lautesse, J.L. Laville, L. Lebreton, C. Le Brun, A. Le Fèvre, R. Legrain, M. Louvel, M. Mahi, N. Marie, T. Nakagawa, L. Nalpas, A. Ouatizerga, M. Parlog, J. Péter, E. Plagnol, E. Pollacco, A. Rahmani, R. Régimbart, M. Reposeur, M. F. Rivet, E. Rosato, F.Saint-Laurent, M. Squalli, L. Tassan-Got, C. Volant, J.P. Wieleczko, A. Wieloch, K. Yuasa-Nakagawa

March1995

LPCC 95-06

Contribution given at the XXXIII[rd] International Winter

Meeting on Nuclear Physics, Bormio, Italy, 23-28 january 1995.

INSTITUT NATIONAL
DE PHYSIQUE NUCLEAIRE ET DE PHYSIQUE DES PARTICULES

CENTRE NATIONAL DE LA RECHERCHE SCIENTIFIQUE

INSTITUT DES SCIENCES
DE LA MATIERE ET DU RAYONNEMENT

UNIVERSITÉ DE CAEN

Téléphone : 31 45 25 00
Télécopie : 31 45 25 49

EVOLUTION OF REACTION MECHANISMS IN SYMMETRICAL NUCLEUS-NUCLEUS COLLISIONS AS A FUNCTION OF THE TOTAL MASS OF THE SYSTEM FROM 25 TO 74 MeV/u

V. Métivier [1], R. Bougault [1], J.L. Charvet [2], D. Cussol [1], D. Durand [1], R. Laforest [1], J.F. Lecolley [1], O. Lopez [1], J.C. Steckmeyer [1], B. Tamain [1], E. Vient [1], G. Auger [4], Ch.O. Bacri [3], A. Benkirane [4], J. Benlliure [4], B. Berthier [2], B. Borderie [3], P. Box [3], R. Brou [1], Y. Cassagnou [2], A. Chbihi [4], J. Colin [1], R. Dayras [2], E. De Filippo [2], A. Demeyer [5], P. Ecomard [4], P. Eudes [6], A. Genoux-Lubain [1], D. Gourio [6], D. Guinet [5], L. Lakehal-Ayat [3], P. Lautesse [5], J.L. Laville [6], L. Lebreton [5], C. Le Brun [1], A. Le Fèvre [4], R. Legrain [2], M. Louvel [1], M. Mahi [1], N. Marie [4], T. Nakagawa [1], L. Nalpas [2], A. Ouatizerga [3], M. Parlog [3], J. Péter [1], E. Plagnol [3], E. Pollacco [2], A. Rahmani [6], R. Régimbart [1], T. Reposeur [6], M.F. Rivet [3], E. Rosato [1], F. Saint-Laurent [4], M. Squalli [3], L. Tassan-Got [3], C. Volant [2], J.P. Wieleczko [4], A. Wieloch [1], K. Yuasa-Nakagawa [1]

1) LPC, IN2P3-CNRS, ISMRA et Université, 14050 CAEN CEDEX, France
2) CEA, DAPNIA/SPhN, CEN Saclay, 91191 GIF SUR YVETTE CEDEX, France
3) Institut de Physique Nucléaire, IN2P3-CNRS, 91406 ORSAY CEDEX, France
4) GANIL, CEA et IN2P3-CNRS, B.P. 5027, 14021 CAEN CEDEX, France
5) IPN Lyon, IN2P3-CNRS et Université, 69622 VILLEURBANNE CEDEX, France
6) SUBATECH, IN2P3-CNRS et Université, 44072 NANTES CEDEX 03, France

Abstract

Ar+KCl and Xe+Sn systems have been studied with Indra from 25 to 74 MeV/u. It is shown that binary dissipative processes are dominant in every case. Excitation energies exceeding 10 MeV/u are reached for primary outgoing partners. Their decay takes place by particle and IMF emission. The corresponding mean kinetic energies can be understood in a statistical model approach and the role of expansion energy is negligible up to 50 MeV/u bombarding energy.

1 - Introduction

Reaction mechanisms in heavy ion induced reactions are clearly identified at low bombarding energy [1,2]. Complete fusion takes place for central collisions if the product Z_1Z_2 of the atomic numbers of the initial partners is lower than 2500. On the other hand, for larger Z_1Z_2 values, the main outgoing channel corresponds to deep inelastic mechanism. When increasing the incident bombarding energy in the intermediate energy domain (10-100 MeV/u), many results concerning central collisions have been interpreted in the incomplete fusion picture [3]. It is generally observed that up to 35 MeV/u,

incomplete fusion can be unambiguously recognized. At larger energies the fusion component seems to vanish but this result has often been linked either to the maximum excitation energy which can be sustained by a nucleus, or to the opening of new decay channels. Only in some cases, deep inelastic processes have been recognized and analyzed [4-7], and the repartition of the total cross section between both mechanisms is generally unknown. This situation is rather dangerous since many data are analyzed, assuming a priori that incomplete fusion is the dominant channel for violent collisions. It is for instance the case when Intermediate Mass Fragment (IMF) production is attributed to hot nucleus decay, without testing whether they originate from a definite source [8]. Generally, such an assumption is performed because many bodies are involved in the exit channel and it is difficult to disentangle entrance and exit step effects. Moreover, for large energy deposits, these two steps can overlap in time as revealed by the occurrence of pre-equilibrium emission.

In order to progress towards a complete description of the collision, it is necessary to perform experiments as exclusive as possible, in which both the nature and kinematical properties of all the outgoing products are recognized. Indra [9] is a 4π device ensuring this objective for charged products. Because it consists of many modules involving gas chambers, silicon detectors and ICs scintillators with a large geometrical efficiency, it is able to detect and analyze in nature, energy and emission angle any nucleus from Z=1 to 50, on an energy range from 1 MeV to several GeV. We present in this paper results concerning nearly symmetrical systems (Ar+KCl and Xe+Sn) over an incident energy range extending between 25 to 74 MeV/u. After a short description of the experiment (section 2), we will first present a general view of the reaction in section 3. Then we will focus (section 4) on fusion events leading to evaporation residues. They have been recognized with a limited cross section for the Ar+KCl system below 40 MeV/u and for Xe+Sn below 30 MeV/u. The corresponding excitation energies (or temperatures) are quite large (6-8 MeV/u) and the survival of such very excited nuclei is a constraint for the statistical models describing their decay.

For any reaction, whatever the bombarding energy, dissipative binary mechanisms represent the largest proportion of the cross section for violent collisions. Section 5 is devoted to these events. In the case of the Ar+KCl system, which is a light system, such a result is strongly different from what is observed at low incident energy, since in this case, fusion is dominant. It is compared with predictions based on Landau-Vlasov calculations. The excitation energies deposited into the fragments during the deep inelastic process are rather large ($\geq$ 7-10 MeV/u). Nevertheless, for the light Ar+KCl system, the two outgoing products decay takes place mostly through light charged particle emission (Z=1 and 2). On the contrary, in the case of the heavier Xe+Sn system,

the two primary fragments decay by multifragment emission. These properties are established and discussed in section 5. Section 6 is a general conclusion in which the evolution of reaction mechanisms with total mass and bombarding energy is discussed for symmetrical systems.

2 - Description of the experiment

Two systems have been studied at various bombarding energies : Ar+KCl at 32, 40, 52 and 74 MeV/u ; Xe+Sn at 25, 32, 40 and 50 MeV/u. The KCl target was deposited on a thin 20 $\mu g/cm^2$ carbon backing. The natural Sn target was self supporting. Their thicknesses were 410 $\mu g/cm^2$ for KCl and 350 $\mu g/cm^2$ for Sn. The beam intensity was maintained quite low (below one electrical nanoampere), in order to limit the pile-up rate below 10^{-4}. Indra was triggered if at least three modules fired in

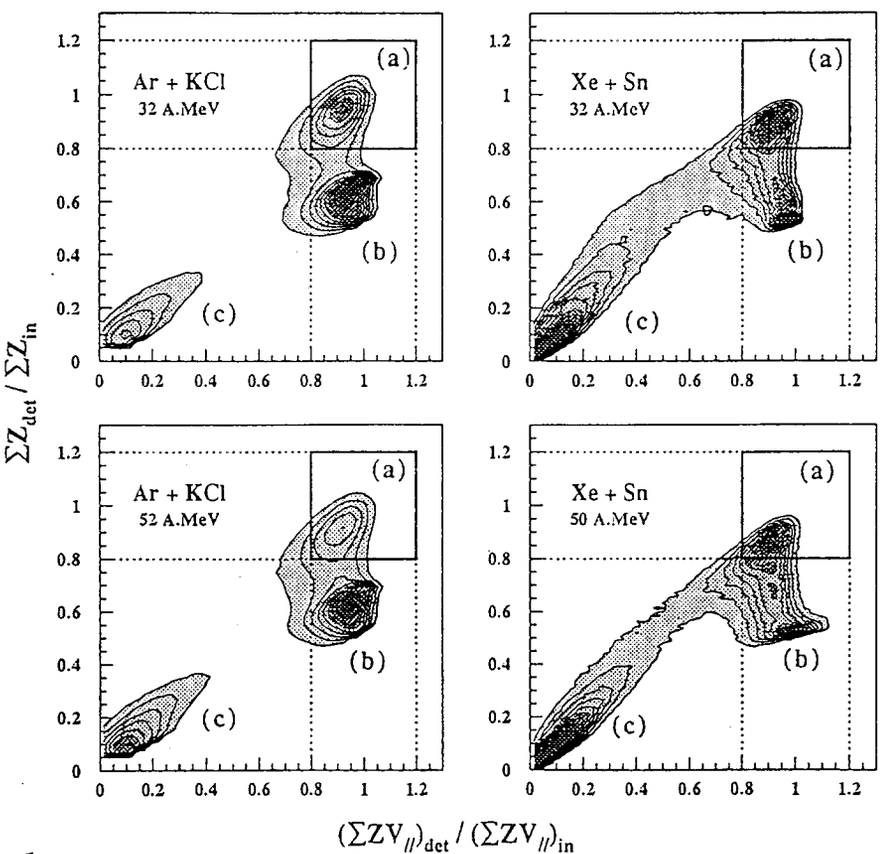

Figure 1

"Complete events" selection : total-detected-charge versus total-detected-linear-momentum plot. The quoted quantities are normalized to their expected values. Properly detected (complete) events are selected as indicated by the square in the upper right corner of each plot (zone (a)). Zones (b) and (c) correspond to peripheral or semi-peripheral events for which the quasi-target (zone (b)) or both quasi-projectile and quasi-target (zone (c)) have been lost due to the detector acceptance (geometrical and threshold).

coincidence. The corresponding counting rate was about 200 s^{-1}. The beam was continuously registered in a Faraday cup and the acquisition dead time was also continuously measured. The stability of the electronics was monitored with pulsers or lasers (for ICs counters) and the energy calibrations were performed by using both ions and light charged particles elastic scattering. Details on all these procedures can be found in ref. 9.

3 - General insight of the results

When analyzing experiments performed with a 4π device, it is essential to ensure that the detector filter does not affect too much the data. A direct way of testing the performance of the set-up consists in checking the charge and momentum conservation of detected products. This can be done from figure 1 where the total charge and linear momentum detected in a given event for Ar+KCl and Xe+Sn systems are plotted at two bombarding energies. The measured values have been normalized to the expected ones.

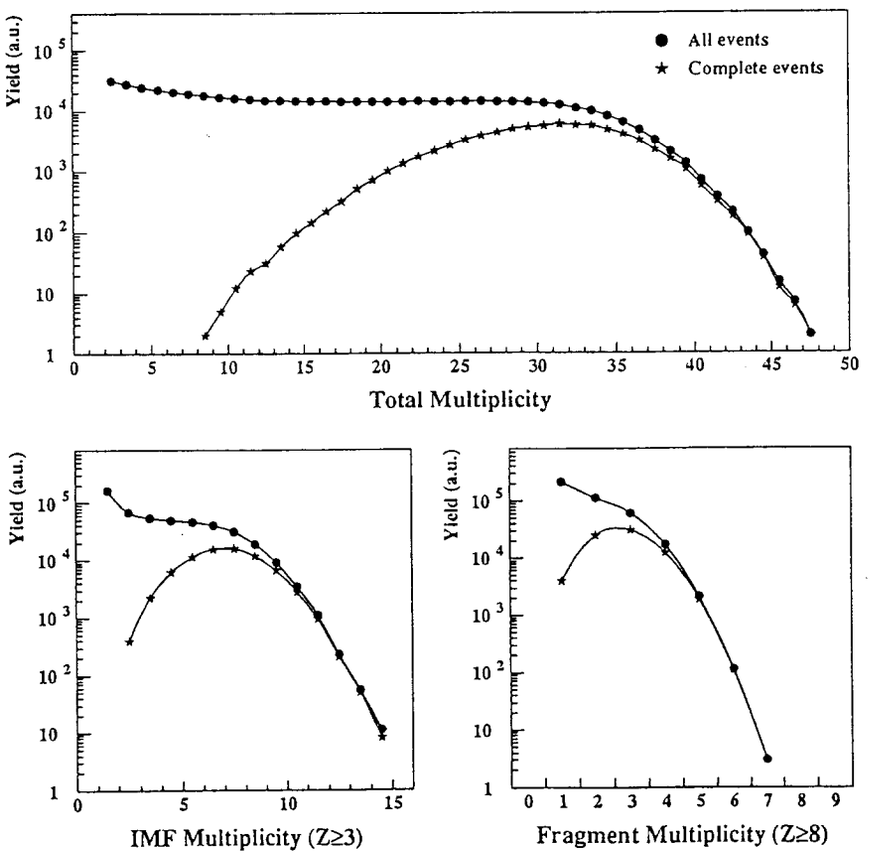

Figure 2

Various multiplicity distributions for the 50 MeV/u Xe+Sn system ; upper : all charged particles ; bottom : IMF (Z≥3) or fragments (Z≥8). The distributions are plotted for all events (points) and for complete events (stars : zone (a) in figure 1). No renormalization is applied.

Properly measured (complete) events are located aroung the points of coordinates (1, 1) in fig. 1. It turns out that many events lie outside this range but it has been shown in a simulation performed in ref. 10 that they are due to peripheral or semi-peripheral collisions for which the quasi-target (zone b), or both heavy partners (zone c) have been missed due to the threshold and to the forward Indra beam hole. In the case of the Ar+KCl system one has also to add the fact that some events are due to reactions induced on the carbon backing (this difficulty does not exist for the self supporting Sn target). Backing events are however all rejected if one asks for more than 80% of the total expected charge and linear momentum. "Complete events" correspond to about 15% of the total reaction cross section both for Ar+KCl and Xe+Sn systems. They are mainly due to central or semi-central collisions, as can be deduced from figure 2 in which various multiplicity distributions are plotted : total multiplicity for charged particles, multiplicity for Intermediate Mass Fragments (IMF: $Z \geq 3$), multiplicity for Fragments ($Z \geq 8$). In any case, the "complete events" requirement corresponds to a selection of all violent reactions (large multiplicity values) , and to a strong suppression of peripheral

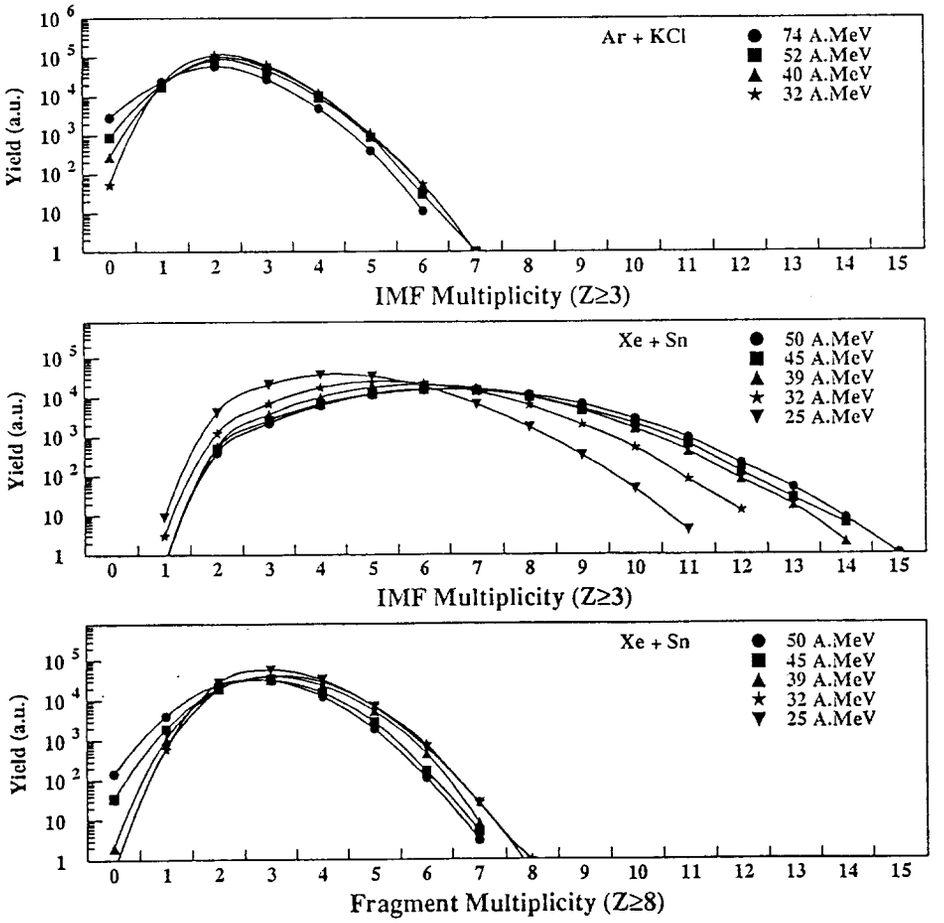

Figure 3

IMF and fragment multiplicity distributions for various systems and bombarding energies ; the "complete events" requirement is applied.

ones. More information can be obtained from figure 2 : large IMF and fragment multiplicities are reached for the quoted system. This is a quite general remark which applies to the Xe+Sn system and to a lesser extent to the Ar+KCl one, whatever the bombarding energy is. Figure 3 gives an indication of this feature : most of central reactions correspond to at least 2 IMF in any case. Few complete events are associated with one single IMF only for Ar+KCl : in the next section, we will test to which extent they correspond to an incomplete fusion process leading to a single residue.

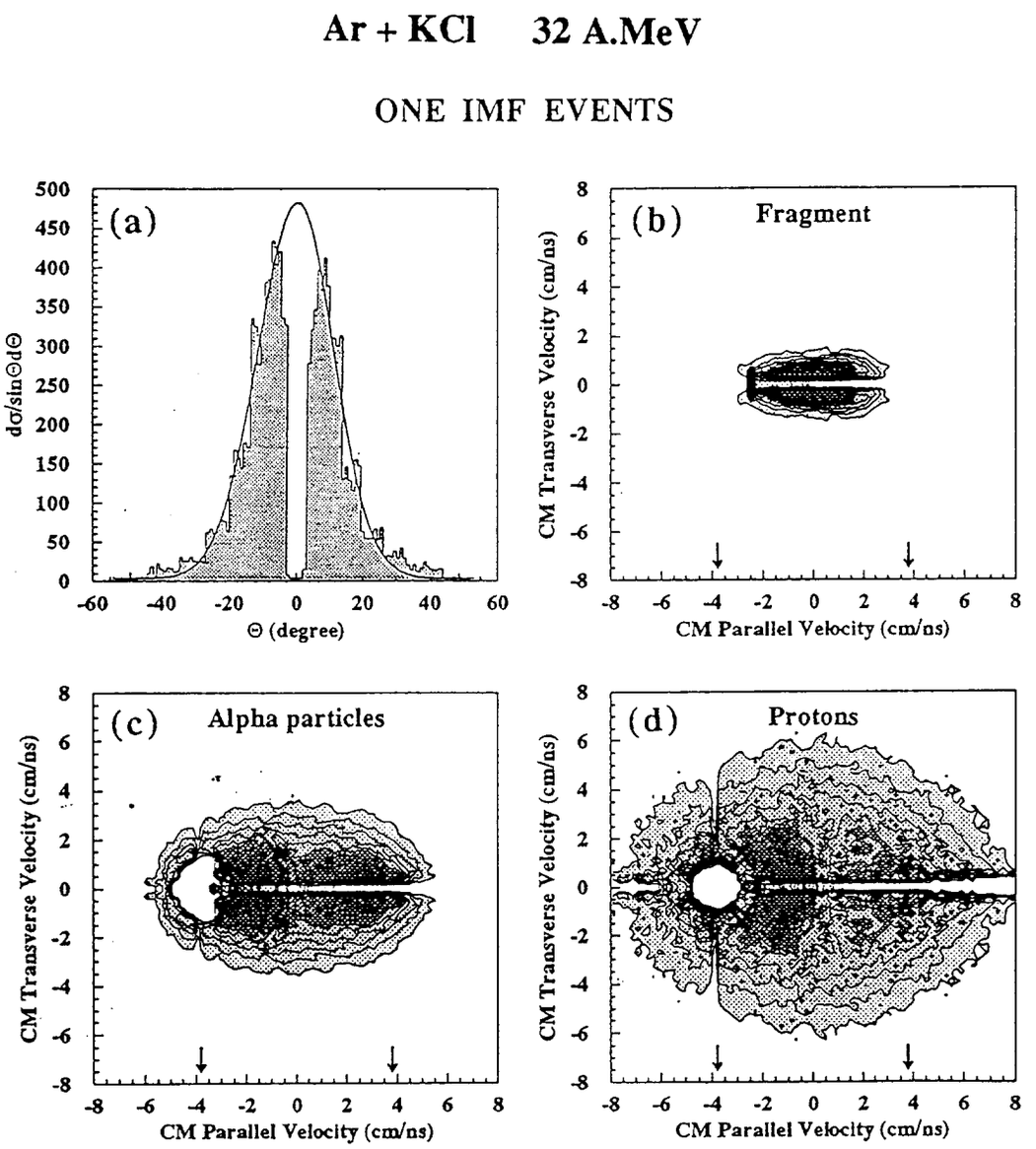

Figure 4

"One IMF" events properties. Part (a) : laboratory frame IMF angular distribution *; part (b) : IMF invariant cross section in the $V_{//}$ - $V_{\perp}$ plane ; the arrows indicate the projectile and target velocities ; part (c) (d) : coincident alpha particles (protons) invariant cross sections in the $V_{//}$ - $V_{\perp}$ plane.*

4 - "One IMF" events

"One IMF" events have been registered for the Ar+KCl system. Their cross section is 70 mbarns, including inefficiency effects. None of them have been recovered in the Xe+Sn case. At limited bombarding energy (32 MeV/u), many of these events (see below) are due to fusion (the single IMF is the fusion residue), but it turns out that binary reactions play also a role. Figure 4 gives several indications on these features. The forward peaked laboratory angular distribution (fig. 4-a) is expected for fusion residues ; similarly the invariant cross section in the $V_{//}$ - $V_{\perp}$ plane exhibit a single source pattern, and the extracted source velocity is at rest in the c.m. system (figure 4-b). However the isocontours are quite elongated. Similarly, the alpha and to a less extend proton plots (figures 4-c-d) exhibit non equilibrium features. The evolution of the IMF contour plots with bombarding energies is spectacular. One sees in figure 5 that they correspond to a

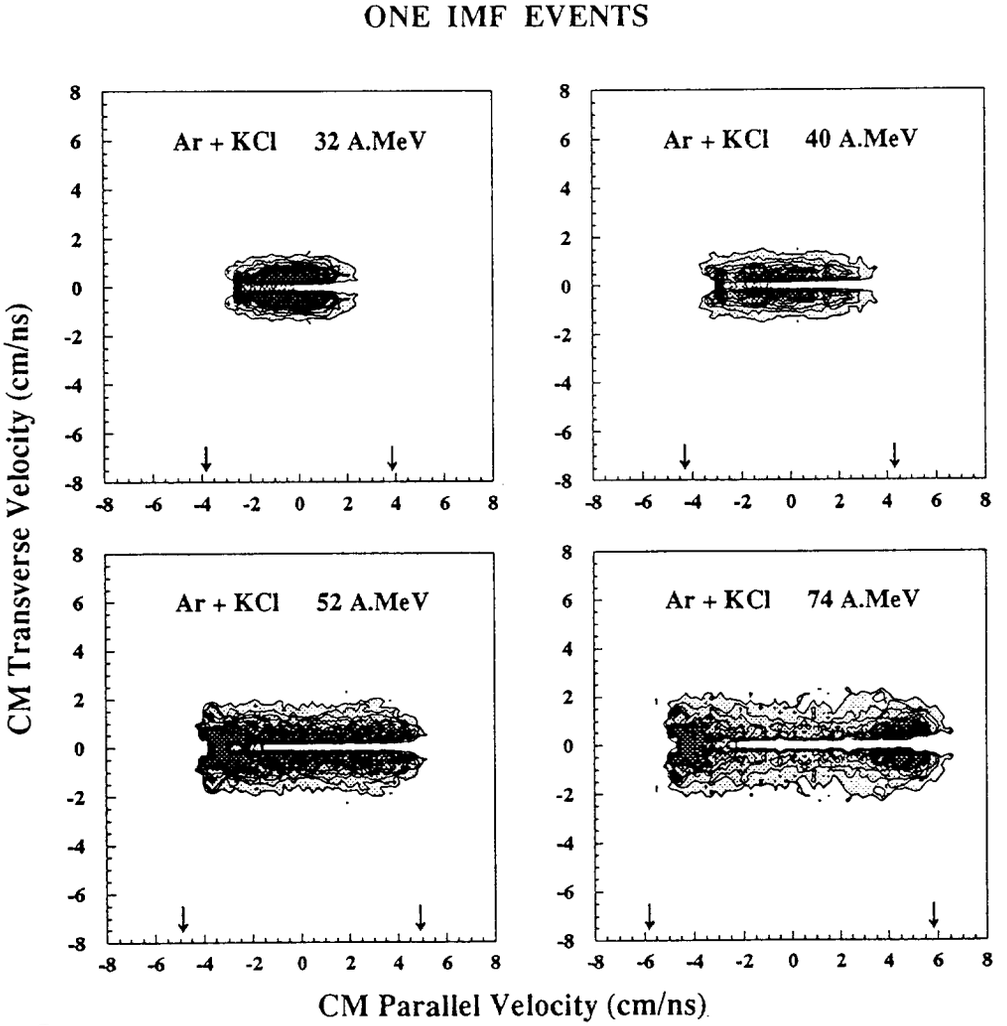

Figure 5
IMF invariant cross section in the $V_{//}$ - $V_{\perp}$ plane for the Ar+KCl system at various bombarding energies.

binary process for which one of the outgoing partners has been completely fragmented in $Z \leq 2$ particles. The elongated shape of the $V_{//}$ - $V_{\perp}$ plot of figure 4-b results from the fact that such "one IMF" events also exist at 32 MeV/u : a detailed analysis revealed that they represent in this case about 1/3 of the total cross section for "one IMF" production.

No "one IMF" event (only one product with $Z \geq 3$) has been detected for the Xe+Sn system since in this case, fusion residues are expected to be heavier. And indeed, "one Fragment" events (only one product with $Z \geq 8$) have been detected and identified as fusion events leading to a single residue. However, the corresponding cross section is quite low : below 10 mbarns at 25 MeV/u.

5 - The dominant role of two source events

The dominance of two sources reactions has been observed from this experiment both for the Ar+KCl and Xe+Sn systems. Our purpose in this section is to establish this feature. A first indication can be obtained from figure 6 in which two $V_{//}$ - Z plots are shown : for each event, one has diagonalized the momentum tensor in order to extract the main axis ; $V_{//}$ is the velocity component on this main axis for any IMF (or fragment) belonging to the event. Z is the corresponding charge. In figure 6-a, any IMF ($Z \geq 3$) has been considered. In figure 6-b only the two heaviest ones have been retained. It turns out that most of the considered products can be attributed to one forward source (projectile-like fragment) and a backward one (target-like fragment). The two arrows indicate the initial projectile and target velocities in the center of mass frame. The relative velocities between the selected projectile-like and target-like sources correspond to some dissipation since most peripheral collisions have been eliminated by the "complete event " requirement explained in section 3 (figure 1). However, they are generally much larger than the expected values for coulomb repulsion (about 2.5 cm/ns) and only few events can result from a fusion nucleus decay.

Hence it is justified to reconstruct the initial projectile and target-like products. We did it by attributing the various IMF (or fragments) of a given event to the projectile-like or target-like sources. The mathematical method which has been used to optimize this sharing consists in the search for the maximum value of the thrust :

$$T = \frac{\left| \Sigma \vec{p}_i \right| + \left| \Sigma \vec{p}_j \right|}{\Sigma \left| \vec{p}_k \right|}$$

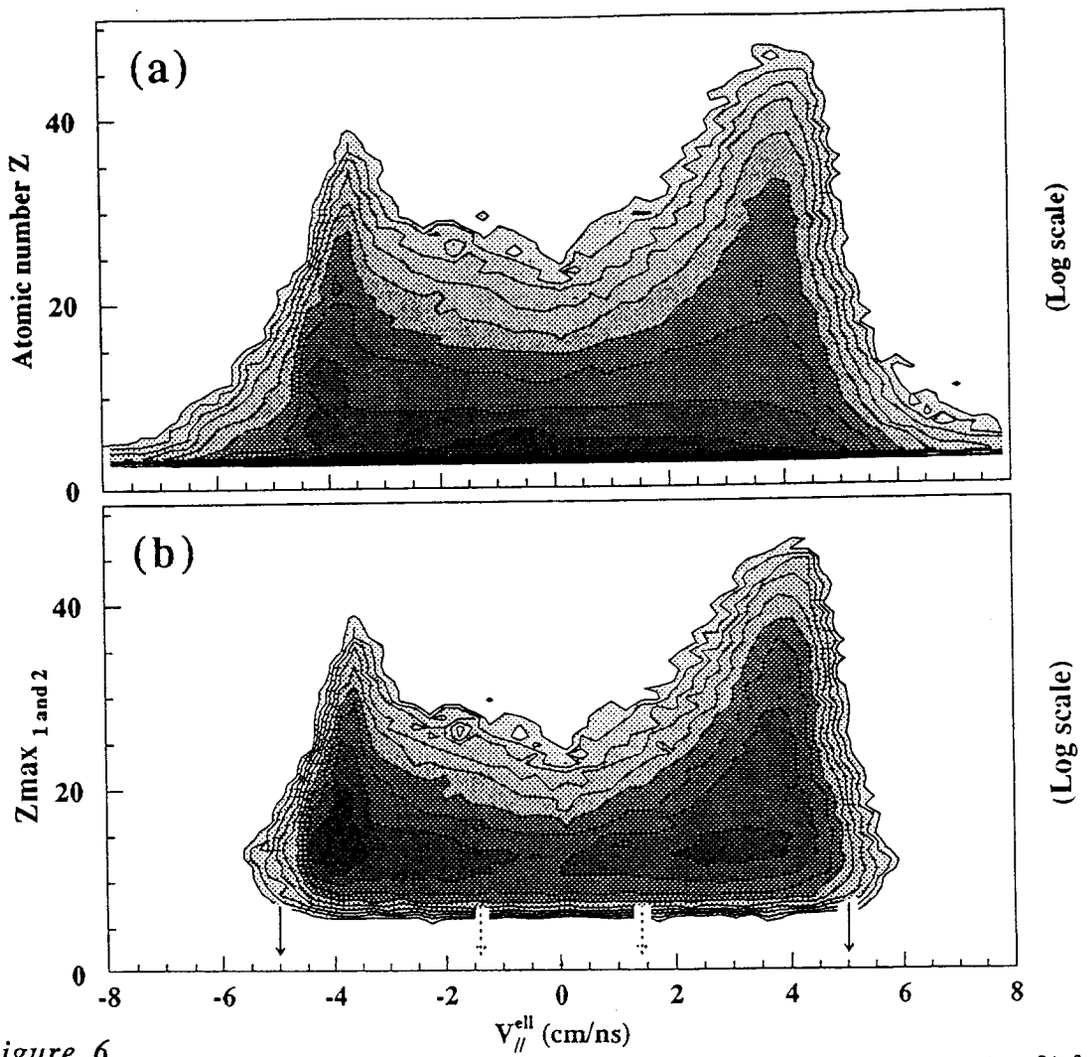

Figure 6

$V_{//}$ - Z plots for various IMF belonging to "complete events" (see section 3) for the Xe+Sn system at 50 MeV/u. In part (a) of the figure any IMF has been retained. In part (b), only the two heaviest of a given event are retained. Most events exhibit a two source behaviour and only few of them can correspond to fusion.

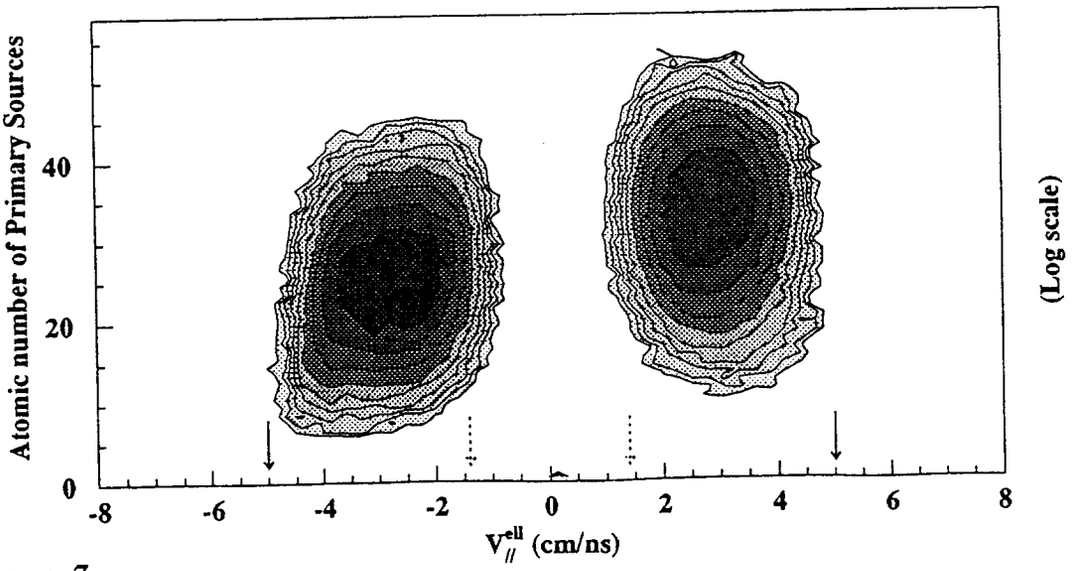

Figure 7

$V_{//}$ - Z plot of the primary sources reconstructed by maximizing the thrust for each event (see text) - Xe+Sn system at 50 MeV/u.

In the numerator, each summation includes IMF which have been attributed to a definite source. The denominator is simply a scaling factor. The result of such a procedure is shown in figure 7 which is a $V_{//}$ - Z plot for the reconstructed sources. They are now quite well separated.

In figure 8, one can get a better insight of the above procedure. For each charged product belonging to a given event, one has plotted the correlation between the

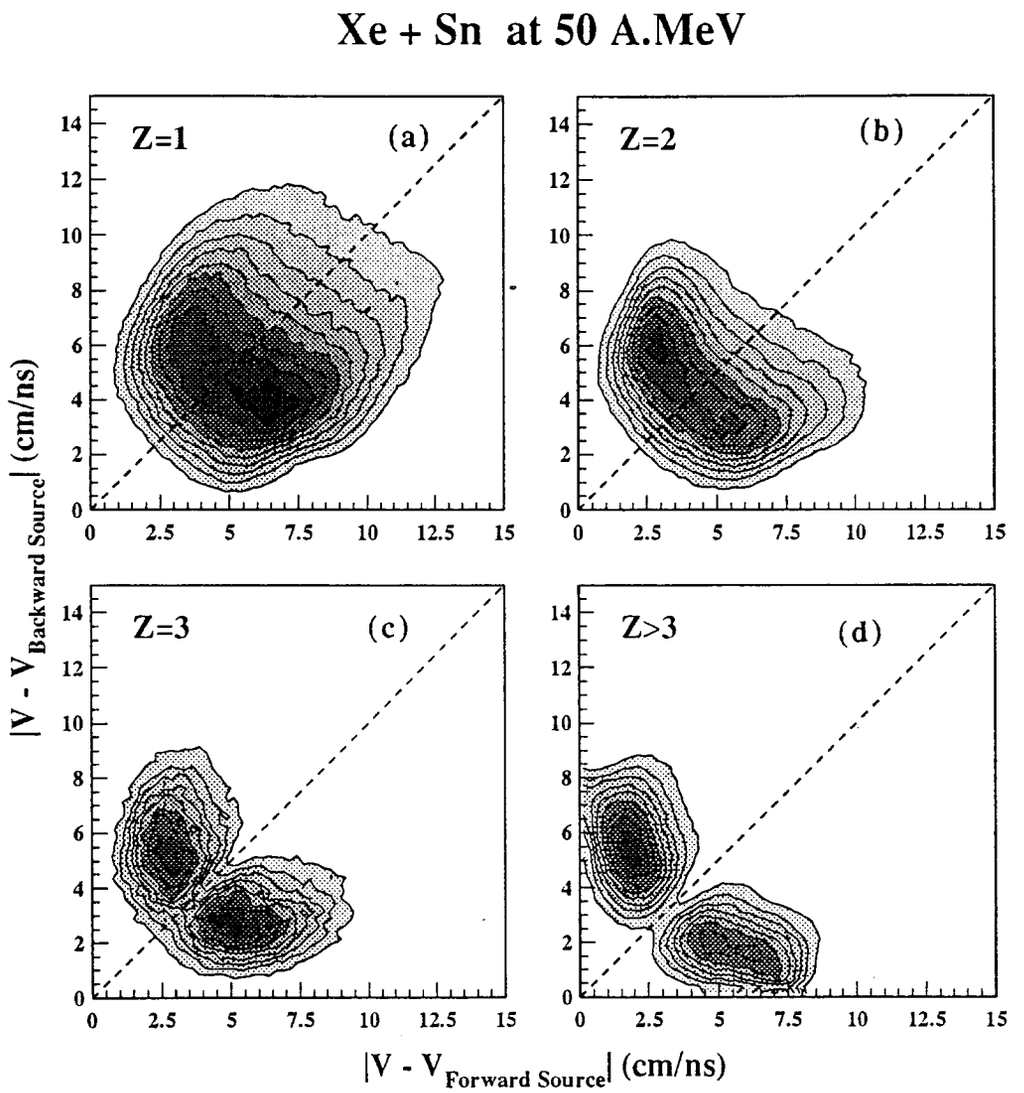

Figure 8

Correlations between the velocities of a given product (Z=1, or 2, or 3, or >3) calculated in the two reference frames associated with the two reconstructed primary sources (see text) for the 50 MeV/u Xe+Sn system.

velocities relative to the two reconstructed sources. It turns out that a given IMF can be generally attributed unambiguously to a given source. The situation is not so clear for the coincident alphas or protons (figures 8 a, b), even if most of the alpha particles exhibit the same behaviour as the IMF (or Fragments).

Such a behaviour has been obtained whatever the bombarding energy for both studied systems : Ar+KCl from 32 to 52 MeV/u and Xe+Sn from 25 to 74 MeV/u. Figure 9 gives another representation of the results : one has plotted the correlation between the relative velocity of the reconstructed sources and the rotation angle of the di-nuclear source system during the reaction . One obtains what is generally called a

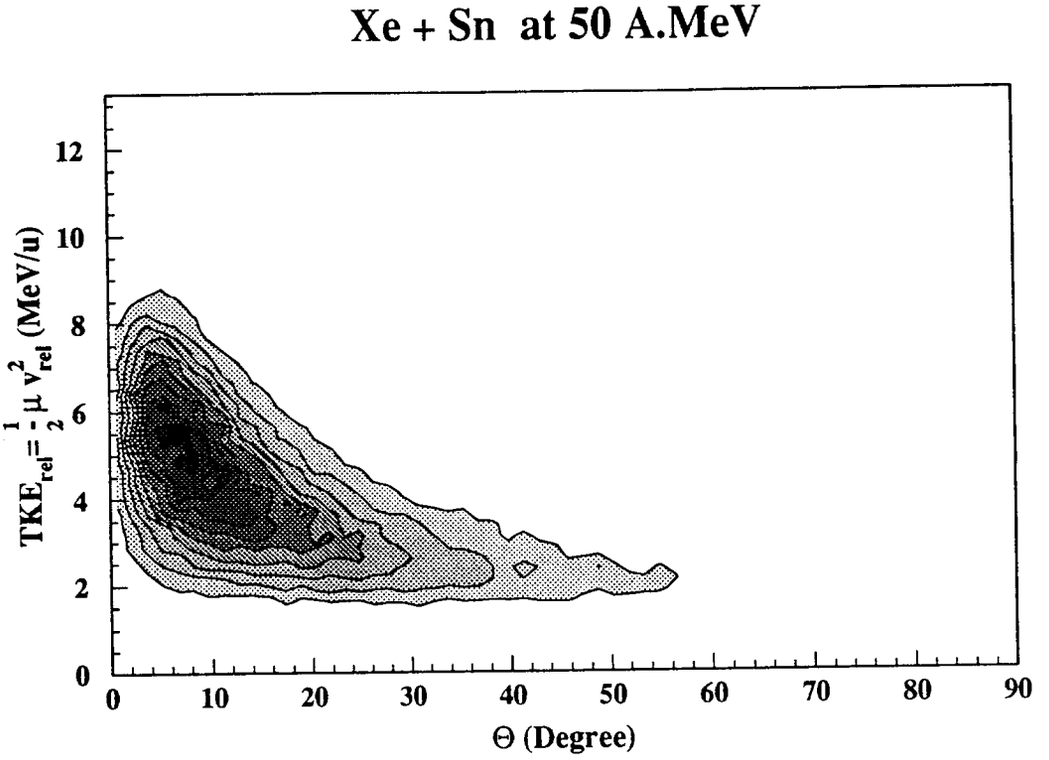

Figure 9
Correlation between the relative velocity (in MeV/u unit) of the reconstructed primary sources and the rotation angle of the di-nuclear source system for the 50 MeV/u Xe+Sn system.

Wilczynski plot at lower bombarding energy : deep inelastic collisions are quite dominant at and above 30 MeV/u for symmetrical systems. For the lightest system (Ar+KCl), this result is different from the known behaviour at lower bombarding energy. It has been however reproduced in Landau-Vlasov calculations [12]. An example is given in figure 10 for the Ar+KCl system at 32 MeV/u. It turns out that fusion takes place for impact parameters lower than 2 fm, which corresponds to a cross section of about 100 mbarns slightly larger than the corresponding experimental value discussed in section 4 . The remaining part of the cross section corresponds to two main bodies events, i.e. to deep inelastic ones.

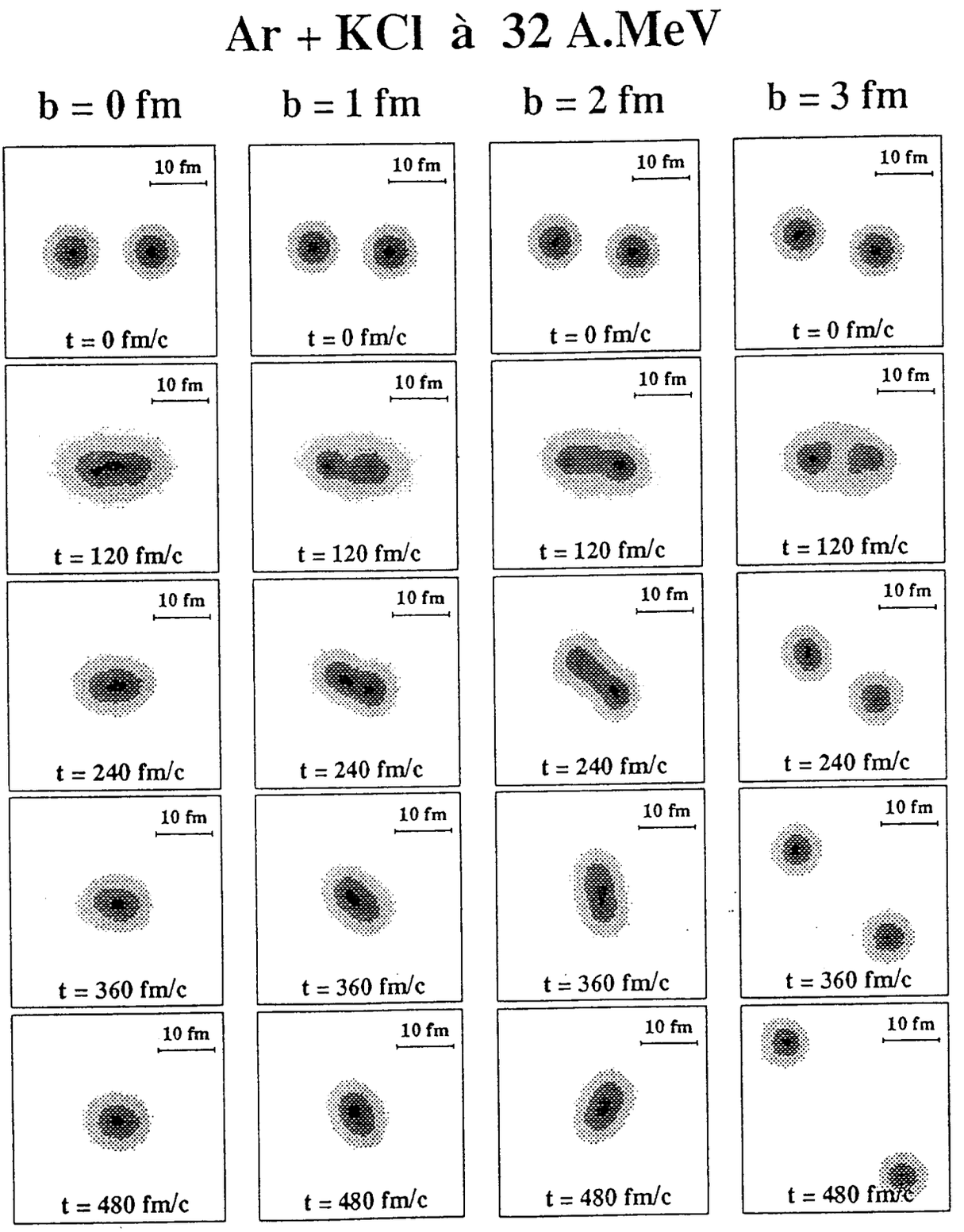

Figure 10

Landau-Vlasov calculations performed for the Ar+KCl system at 32 MeV/u for various impact parameters. Density profiles in the coordinate space are shown as a function of time, for various impact parameters.

Now, it is possible to extract from the data the involved dissipated energies. We have done it in two ways : first, from the relative velocity of the reconstructed sources. This method is quite valid if the process is binary and if pre-equilibrium contributions do not affect significantly the results. Simulations performed with the Eugene code for similar systems indicate that the latter hypothesis is reasonable [7]. The second method consists in calculating on an event by event basis, the difference between the initial available energy and the total kinetic energy removed by IMF (or fragments). This second method holds even if the initial process is not binary (fusion instead of deep inelastic process). It is simply assumed that most of the dissipated energy is removed by light particle ($Z \leq 2$) emission. The correlation between dissipated energy values obtained with the two above methods is shown in figure 11. A reasonable agreement is observed. The dissipated energy distributions (in MeV/u) obtained from the first method are shown in figure 12 for Ar+KCl and Xe+Sn at two bombarding energies. It turns out that larger excitation energies per nucleon are reached at larger bombarding energies and that the distributions extend to similar values whatever the total system mass is. Values exceeding 10 MeV/u are obtained with a sizeable cross section as it has already been concluded for similar systems (Ar+Al and Zn+Ti) [7].

Now, it is interesting to correlate the above dissipated energy values with the coincident light charged particles multiplicities. In figures 13 and 14, it turns out that this

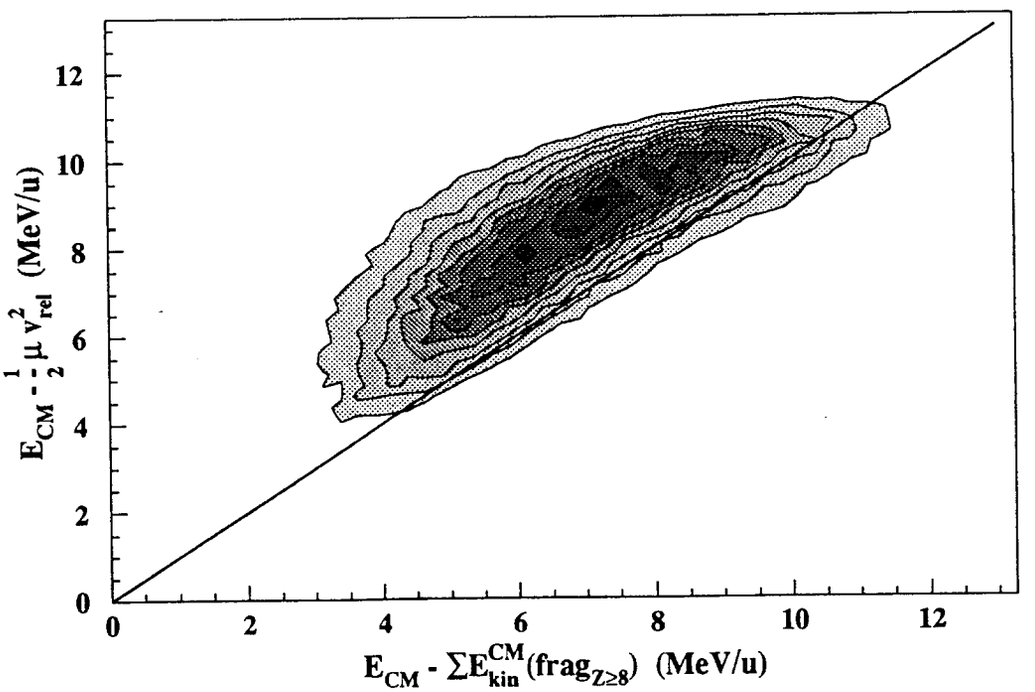

Figure 11

Correlation between dissipated energy values calculated in two ways (see text) for the Xe+Sn system at 50 MeV/u.

correlation is generally strong and that it is independent of the bombarding energy. It is important to stress that, from the experimental point of view, each of the two above quantities is independent from the other one. This feature strongly supports the above procedure for the determination of the dissipated energy. From figure 13, it turns also out that fragment multiplicities observed for the Xe+Sn system do not increase with the dissipated energy. Such a behaviour is also observed in figure 14 for the lighter Ar+KCl system, but in this case it is observed on IMF ($Z \geq 3$), instead of Fragments ($Z \geq 8$). This result has to be compared with a similar feature observed at larger bombarding energies [11]: rise and fall of IMF production ending to complete vaporization of the system if the available energy is sufficient.

A further interesting remark can be obtained from absolute IMF multiplicities. The corresponding mean value is 2 for Ar+KCl, whatever the deposited energy is ; this means that for most events, one gets two IMF (projectile and target remnants) and light charged particles. In the case of Xe+Sn, larger IMF multliplicity values are obtained which means that projectile and target-like nuclei undergo fragment emission or fragmentation. Such remarks could have already been performed from figure 3.

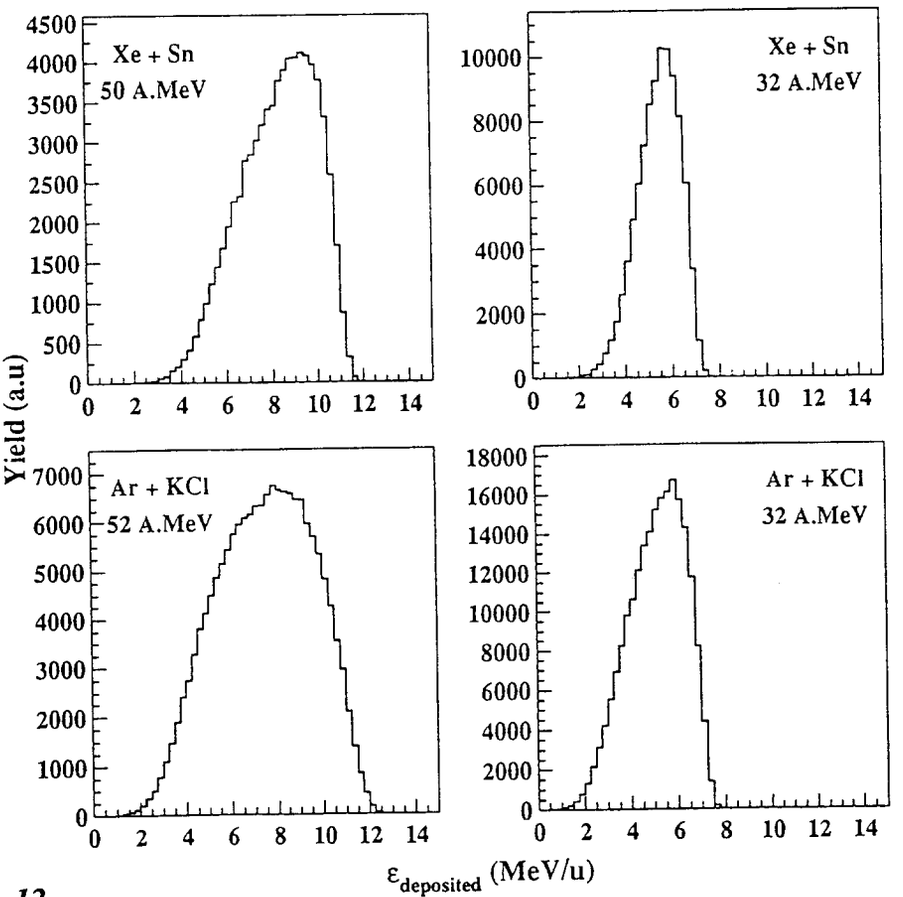

Figure 12

Dissipated energy distributions extracted for several systems at various bombarding energies. The results are independent of the total available mass.

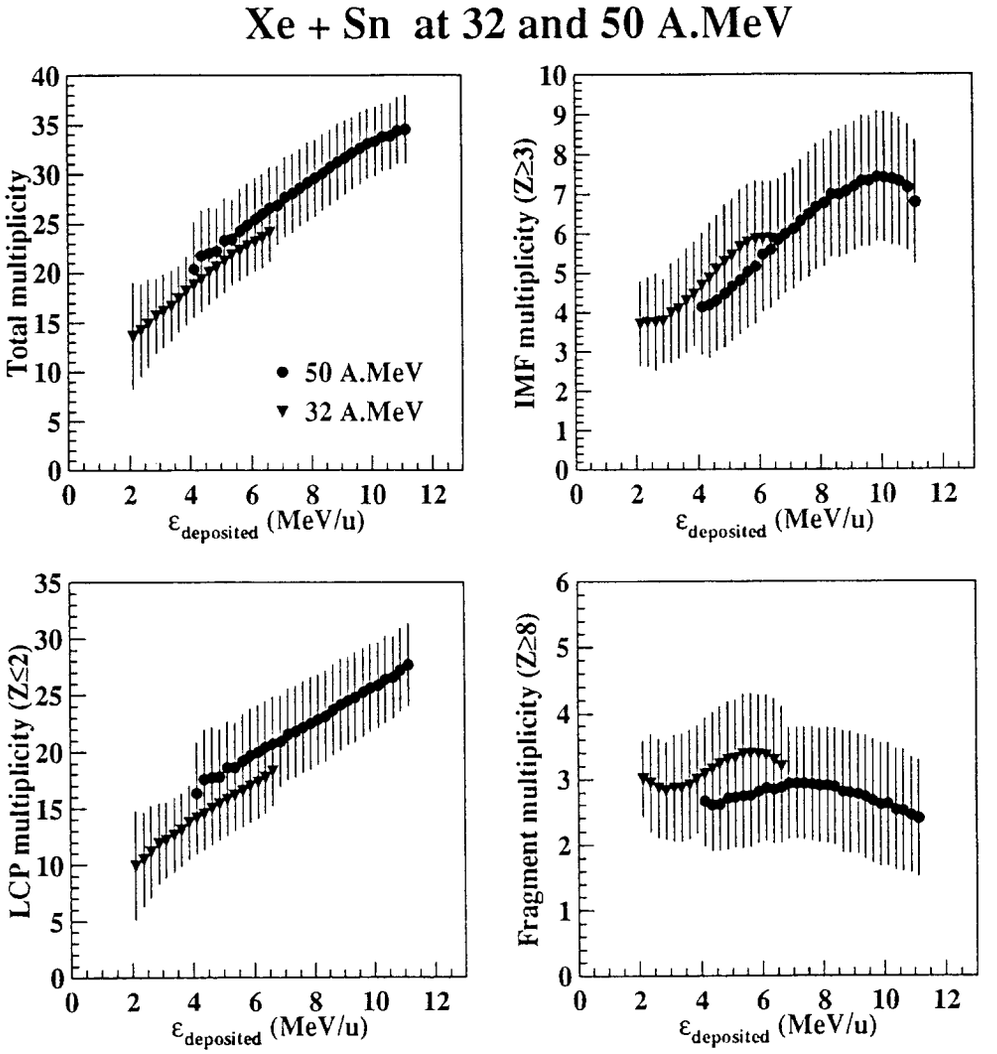

Figure 13
Correlations between light charged particle multiplicities and the dissipated energy extracted as described in the text for the Xe+Sn system at 32 and 50 MeV/u

At this point, one knows that dissipative binary processes play a definite role and that very large excitation energies are deposited into the outgoing primary products. We have seen in figures 13 and 14 that values exceeding 10 MeV/u are reached. It is quite interesting to try to learn about the decay properties of such hot nuclei. Is the stored energy only thermal, or is there some signal for collective modes (compression, expansion) ?

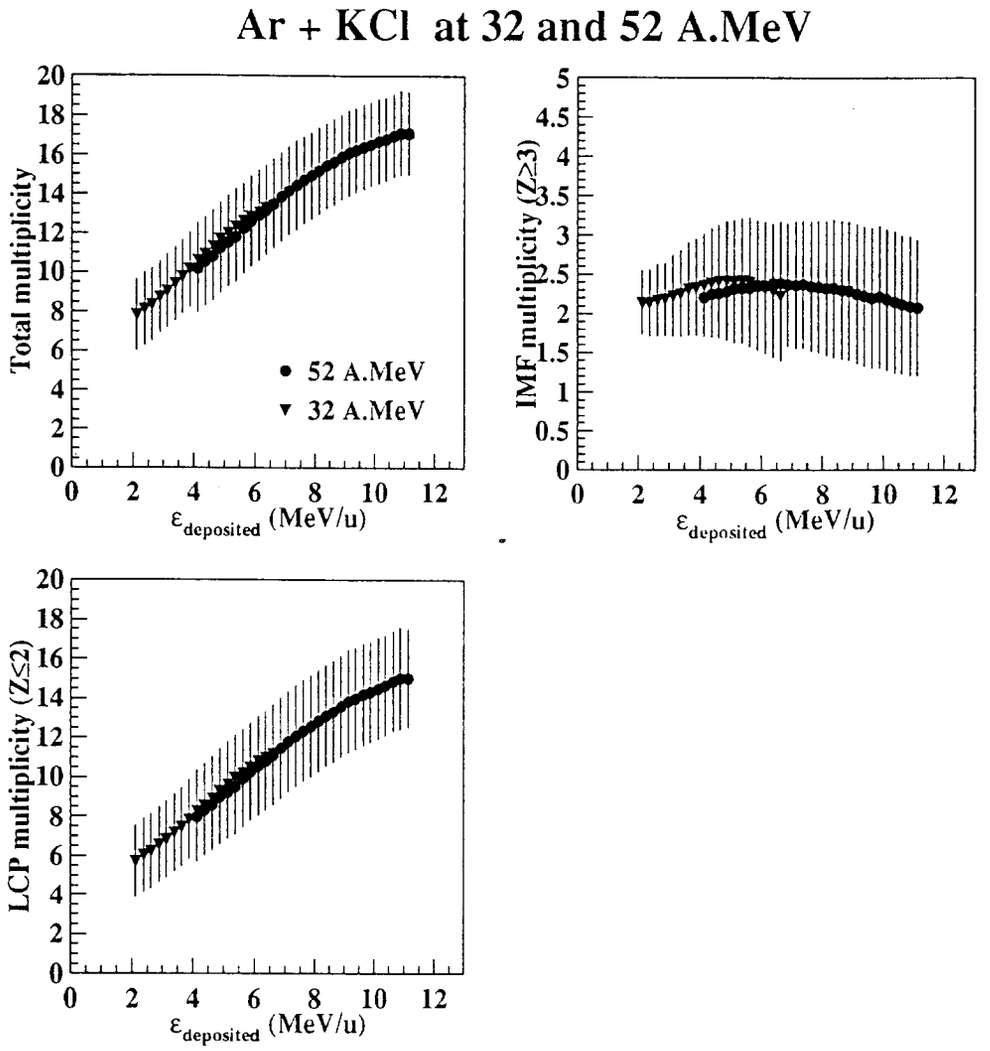

Figure 14
Similar to figure 12 for the Ar+KCl system at 32 and 52 MeV/u.

One can get a first insight of the decay step by looking at figure 15. Various contour plots are shown for alpha particles in the V// - $V_{\perp}$ plane. They correspond to various energy deposit bins (cuts in figure 12 distributions). Remind that $V_{//}$ is defined as the velocity projection on the main axis of the momentum tensor describing each event. It turns out that the binary nature of the process is clearly recognized for the smallest deposited energy ε_{dep}. A second conclusion is that most particles are sequentially emitted after the deep inelastic process step. For increasing ε_{dep} values, the relative velocities between the two sources is reduced, which blurs the picture for deposited energy exceeding 10 MeV/u.

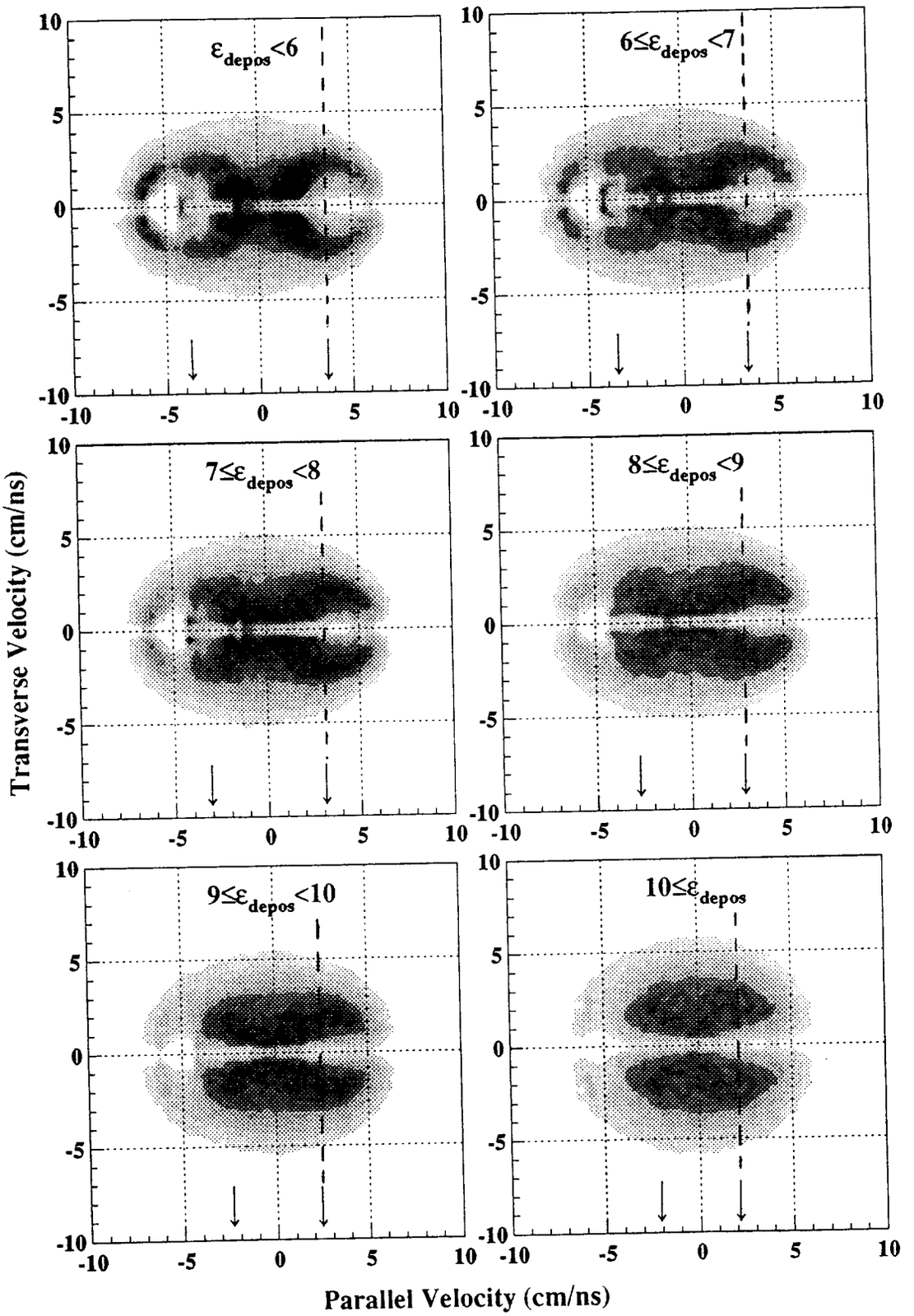

Figure 15

$V_{//}$ - $V_{\perp}$ plots for alpha particles as a function of the extracted deposited energy. The arrows correspond to the primary source velocities. Alpha particles located on the right of the dashed lines have been used to calculate the mean kinetic energies plotted in figure 16. See text.

In order to study the decay of the involved hot nuclei, we have selected in each event one of the two sources (the fastest one, i.e. projectile-like), and in order to eliminate the contribution of the second source and pre-equilibrium particles, one has restricted the subsequent analysis to particles emitted in the forward hemisphere in the projectile-like source frame. In the case of alphas (figure 15), the retained particles are located on the right of the vertical dashed lines drawn in the plots of the figure. This selection has been applied for any decay particle and one has calculated their mean kinetic energy per nucleon in the emitting source frame. In a purely thermal decay, this energy should be related to the sum B+2T of the coulomb barrier and twice the temperature. The results are shown in the left part of figure 16 as a function of the atomic number of the decay particles and for various deposited energy bins. One clearly observes the contribution of the thermal energy on the mean proton kinetic energy, and to a less extent on alpha results. For heavier particles, the thermal energy per nucleon is expected to be reduced because it is divided by the mass number and one expects to observe mainly Coulomb barrier and expansion velocity effects. The fact that the experimental values do not depend on the dissipated energy is a strong indication that for such a system and bombarding energy, the expansion effect is small. The right part of the figure is a typical comparison between experiment and results obtained from a statistical model with sequential emission. Mean kinetic energies are properly reproduced for atomic numbers up to 4, but they are underestimated above. This can be an indication that these products are not sequentially emitted, but further calculations have to be performed in order to understand this feature.

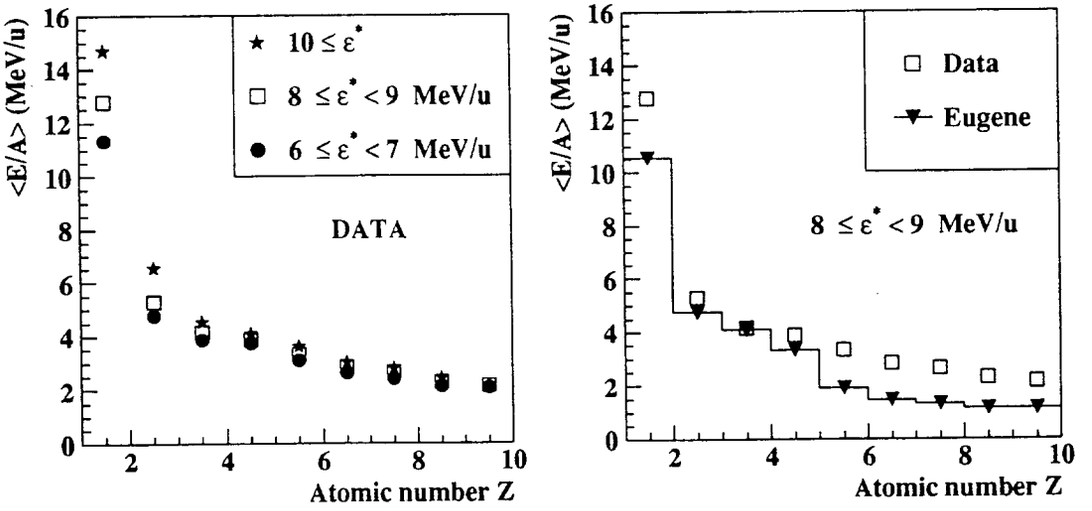

Figure 16

Mean kinetic energy of decay products corresponding to the decay of a hot nucleus as a function of their atomic number. Three deposited energy bins have been selected (left side) and a typical experimental result is compared with a purely statistical model prediction (right side). Xe+Sn system at 50 MeV/u.

6 - Conclusion

In the present experiment, results have been obtained with Indra on reaction mechanisms in violent symmetrical nucleus-nucleus collisions. Complete events have been selected in which more than 80% of total charge and initial linear momentum have been recovered. It has been shown that most central collisions are retained in this way. Most of them do not lead to fusion, but to deep inelastic collisions with two main outgoing products which decay in a second stage. Such a behaviour had already been recognized in ref. 4) and 16) with a limited solid angle set up, and more recently in ref. 7 and 17 with the Nautilus 4π device. In the present work performed with Indra, it has been possible for the first time to reconstruct the primary sources from the kinematical properties of decay IMF. Dissipated energies have been deduced from the relative velocities of the reconstructed primary sources or from the kinetic energy sharing between particles and IMF. Deduced dissipated energy distributions (expressed in MeV/u) are quite similar whatever the total system mass is. Values exceeding 10 MeV/u are reached with sizeable cross sections. The correlation observed between dissipated energy and charged particle multiplicity, the self consistency of the two-source treatment are strong arguments that such results are unbiased. Uncertainties due to preequilibrium emissions can only slightly affect our conclusions. It turns out that the dissipated energy is an increasing function of the bombarding energy. The decay of primary fragments does not give indications of an expansion energy and the bulk of data can be understood in a statistical decay description in which light charged particles and IMF are emitted.

It is however necessary to stress that the above results do not rule out the existence of a small fusion contribution leading to multifragmentation. Such events would correspond to excitation energies larger than 10 MeV/u for Xe+Sn at 50 MeV/u. Moreover, in a given event, few products may result from dynamical effects libe neck emission already recognized by other authors [13-15]. Nevertheless, the present data show that the bulk of data can be undestood in the deep inelastic picture.

Références

1) W.U. Schroder, J.R. Huizenga ; Ann. Rev. Sci. (1977) 465

2) M. Lefort, C. Ngô ; Ann. Phys. Fr. 3 (1978) 5

3) E. Suraud, C. Grégoire and B. Tamain ; Prog. Nucl. Part. Sci. 23 (1989) 357

4) D. Jouan, B. Borderie, M.F. Rivet, C. Cabot, H. Fuchs, H. Gauvin, C. Grégoire, F. Hanappe, D. Gardès, M. Montoya, B. Rémaud and F. Sébille ; Z. Phys. A340 (1991) 63
B. Borderie, M. Montoya, M.F. Rivet, D. Jouan, C. Cabot, H. Fuchs, D. Gardès, H. Gauvin, D. Jacquet, F. Monnet ; Phys. Lett. B205 (1988) 26

5) J.F. Lecolley, L. Stuttgé, M. Aboufirassi, A. Badala, B. Bilwes, R. Bougault, R. Brou, F. Cosmo, J. Colin, D. Durand, J. Galin, A. Genoux-Lubain, D. Guerreau, D. Horn, D. Jacquet, J.L. Laville, F. Lefebvres, C. Le Brun, J. Lemière, O. Lopez, M. Louvel, M. Mahi, M. Morjean, C. Paulot, A. Péghaire, N. Prot, G. Rudolf, F. Scheibling, J.C. Steckmeyer, B. Tamain, S. Tomasevic ; Phys. Lett. B325 (1994) 317

6) G. Casini, A.A. Stefanini, M. Bini, P.R. Maurenzig, A. Olmi, G. Poggi et al ; Phys. Rev. Lett. 67 (1991) 3364
G. Casini, P.G. Bizzeti, P.R. Maurenzig, A. Olmi, A.A. Stefanini et al ; Phys. Rev. Lett. 71 (1993) 2567

7) J.C. Steckmeyer, A. Kérambrun, J.C. Angélique, G. Auger, G. Bizard, R. Brou, C. Cabot, Y. Cassagnou, E. Créma, D. Cussol, D. Durand, Y. El Masri, P. Eudes, M. Gonin, K. Hagel, Z.Y. He, C. Lebrun, R. Legrain, A. Péghaire, J. Péter, R. Régimbart, E. Rosato, F. Saint-Laurent, B. Tamain, E. Vient and R. Wada ; this conference

8) K. Hagel, M. Gonin, R. Wada, J.B. Natowitz, B.H. Sa, Y. Lou, M. Gui, D. Utley, G. Nebbia, D. Fabris, G. Prete, J. Ruiz, D. Drain, B. Chambon, B. Cheynis, D. Guinet, X.C. Hu, A. Demeyer, C. Pastor, A. Giorni. A. Llères, P Stassi, J.B. Viano, P. Gonthier ; Phys. Rev. Lett. 68 (1992) 2141

9) J. Pouthas et al ; to be published in Nucl. Inst. Meth.

10) E. Plagnol et al ; to be published

11) J. Hubele, P. Kreutz, J.C. Adloff, B. Begemann-Blaich, P. Bouissou, G. Imme, I. Oiri, G.J. Kunde, S. Leray, V. Lindenstruth, Z. Liu, U. Lynen, R.J. Meijer, U. Mildau, A. Moroni,W.F.J. Müller, C. Ngô, C.A. Ogilvie, J. Pochodzalla, G. Raciti, G. Rudolf, H. Sann, A. Schüttauf, W. Seidel, L. Stuttgé, W. Trautmann, A. Tucholski ; Z. Phys. A340 (1991) 263

12) C. Grégoire, B. Remaud, F. Sébille, L. Vinet, Y. Raffray ; Nucl. Phys. A465 (1987) 317

13) J.F. Lecolley, L. Stuttgé, M. Aboufirassi, B. Bilwes, R. Bougault, R. Brou, F. Cosmo, J. Colin, D. Durand, J. Galin, A. Genoux-Lubain, D. Guerreau, D. Horn, D. Jacquet, J.L. Laville, F. Lefebvres, C. Le Brun, O. Lopez, M. Louvel, M. Mahi, C. Meslin, M. Morjean, A. Péghaire, G. Rudolf, F. Scheibling, J.C. Steckmeyer, B. Tamain, S. Tomasevic ; submitted to Phys. Lett. B, preprint LPCC 95-03 (1995)

14) C.P. Montoya, W.G. Lynch, D.R. Bowmann, G.F. Peaslee, N. Carlin, R.T. De Souza, C.K. Gelbke, W.G. Gong, Y.D. Kim, M.A. Lisa, L. Péghaire, M.B. Tsang, J.B. Webster, C. Williams, N. Colonna, K. Hanold, M.A. McMahan, G.J. Wozniak & L.G. Moretto ; Phys. Rev. Lett. 73 (1994) 3070

15) L. Stuttgé, J.C. Adloff, B. Bilwes, R. Bilwes, F. Cosmo, M. Glaser, G. Rudolf, F. Scheibling, R. Bougault, J. Colin, F. Delaunay, A. Genoux-Lubain, D. Horn, C. Le Brun, J.F. Lecolley, M. Louvel, J.C. Steckmeyer, J.L. Ferrero ; Nucl. Phys. A539 (1992) 511

16) M.F. Rivet, B. Borderie, P. Box, M. Dakowski, C. Cabot, D. Gardes, D. Jouan, G. Mamane, X. Tarrago, H. Utsunomiya, Y. El Masri, F. Hanappe, F. Sébille, F. Haddad ; Proceedings of the XXXI International Winter Meeting on Nuclear Physics, 1993, p. 92

17) A. Kérambrun, J.C. Angélique, G. Auger, G. Bizard, R. Brou, A. Buta, C. Cabot, Y. Cassagnou, E. Créma, D. Cussol, Y. El Masri, P. Eudes, M. Gonin, K. Hagel, Z.Y. He, S.C. Jeong, C. Lebrun, R. Legrain, A. Péghaire, J. Péter, R. Régimbart, E. Rosato, F. Saint-Laurent, J.C. Steckmeyer, B. Tamain, E. Vient, R. Wada ; Preprint LPCC 94-14 , Caen 1994.